Journal of ELECTRONIC MATERIALS, Vol. 41, No. 9, 2012
DOI: 10.1007/s11664-012-2154-y

Thermoelectric Figure of Merit Enhancement in Bi_2Te_3-Coated Bi Composites

T.W. LAN,[1,2,3] Y.C. CHEN,[4] J.C. HO,[2] S.G. SHYU,[4,6] and Y.Y. CHEN[2,5,7]

1.—Department of Physics, National Taiwan University, Taipei 106, Taiwan. 2.—Institute of Physics, Academia Sinica, Taipei 115, Taiwan. 3.—Taiwan International Graduate Program, Academia Sinica, Taipei 115, Taiwan. 4.—Institute of Chemistry, Academia Sinica, Taipei 115, Taiwan. 5.—Graduate Institute of Applied Physics, National Chengchi University, Taipei 116, Taiwan. 6.—e-mail: sgshyu@chem.sinica.edu.tw; 7.—e-mail: cheny2@phys.sinica.edu.tw

This study examines the thermoelectric behavior of composites containing hydrothermally processed tellurium-coated bismuth particles of various sizes. Since only a very thin layer of Bi_2Te_3 forms on the particle surface, the high-pressure compacted composite is still dominated by bismuth as the main ingredient (~96% Bi). Thermoelectric figure of merit ZT values are derived from measurements of thermal conductivity, electrical resistivity, and Seebeck coefficient. As expected, a ZT value almost three times higher than that of bismuth is found. This enhancement appears to be caused mainly by lowered thermal conductivity due to the significant number of grain boundaries, short phonon mean free path in the coating layers, and lattice mismatch.

Key words: Thermoelectric figure of merit, thermal conductivity, bismuth, hydrothermal tellurium coating

INTRODUCTION

Thermoelectricity can play a viable role in renewable energy development.[1] A suitable material can provide a thermo-emf (V) through a temperature gradient T produced from natural (solar, geothermal) heat sources or industrial waste heat. As in all types of power production, however, the efficiency of energy conversion is a major concern.[2] In this case, thermoelectric materials are usually evaluated by their dimensionless figure of merit ZT, defined as

$$ZT = \frac{\alpha^2 T}{\rho\kappa} = \frac{\alpha^2 T}{\rho(\kappa_E + \kappa_L)}. \quad (1)$$

The parameters α and ρ are the Seebeck coefficient and electrical resistivity, respectively, and the thermal conductivity κ has an electronic (κ_E) and a lattice (κ_L) contribution.[3]

The Wiedemann–Franz law states that $T/\rho\kappa_E$ is approximately equal to the constant Lorenz number.[4,5] Consequently, research efforts to increase ZT mostly focus on reduction of the lattice thermal conductivity.[4] Indeed, a phonon glass–electron crystal model proposed by Slake[3] has been used to improve the thermoelectric properties of filled skutterudites,[6,7] which contain rattler atoms in the voids of their cage-like structure. Other approaches incorporate nanoparticles into a bulk matrix[2,8] to induce additional phonon scattering as well as to benefit from quantum confinement.[1,9–11]

Relevant to this work are earlier studies on synthesis of thermoelectric composites with coated particles as building blocks;[12] For example, bulk samples were prepared from fine Bi_2Te_3 particles via a hydrothermal alkali-metal-salt coating process.[13] The alkali metal modifies grain boundaries, which in turn decreases the lattice thermal conductivity. Unfortunately, the grain boundary effect raises the electrical resistivity, resulting in an overall negative ZT modification. Such a disadvantageous side-effect appears to have been reversed in our case study. Pure bismuth particles are thinly coated hydrothermally with tellurium. Following

J.C. Ho—Visiting from Wichita State University, Wichita, KS, USA.
(Received November 15, 2011; accepted May 24, 2012; published online June 15, 2012)

high-pressure compaction, the composite is still dominated by bismuth as the main ingredient, but significantly improved *ZT* values are found from measurements of the individual parameters in Eq. 1.

EXPERIMENTAL PROCEDURES

Commercial bismuth powders have nominal size of 10 μm to 150 μm. Using 325 or 400 mesh sieves, particles of 36 μm to 45 μm or less than 36 μm were obtained. These were processed into tellurium-coated bulk samples, designated as A (10 μm to 150 μm), B (36 μm to 45 μm), and C (less than 36 μm), respectively. An uncoated bismuth composite (10 μm to 150 μm) serves as a reference.

Each set of starting bismuth particles was coated hydrothermally with tellurium at atomic ratio of Bi:Te = 20:1. The powders were then hot compressed (CARVER, 15H-12) into bulk composites at 260°C under uniaxial pressure of 685 MPa for 30 min, reaching 98.9% to 99.8% of the density of bulk bismuth (9.79 g/cm^3) as listed in Table I. For stress relief and removal of any surface oxide, 2-h post-annealing was carried at 200°C out under a gas mixture of 5% H_2 and 95% N_2. The annealing also helped appreciably lower the electric resistivity, e.g., for sample A, from 34.5 $\mu\Omega$ m to 3.3 $\mu\Omega$ m.

RESULTS AND DISCUSSION

Figure 1 shows x-ray diffraction patterns of tellurium-coated bismuth powders (10 μm to 150 μm) prepared by the hydrothermal process. In addition to bismuth, a small amount of Bi_2Te_3 can be clearly identified through its distinctive peaks. Obviously, tellurium has reacted with bismuth to form thin layers of Bi_2Te_3 on the powder surface. This is corroborated by the scanning electron micrographs of compacted composite in Fig. 2a, where Bi_2Te_3 layers are also observable. Energy-dispersive x-ray mappings in Fig. 2b further reveal the elemental distributions, with tellurium residing along the grain boundaries. Inductively coupled plasma optical emission spectrometry yields a Bi:Te atomic ratio of 27:1. The discrepancy between this ratio and the initial value of 20:1 indicates that some tellurium loss may have occurred during the hydrothermal coating process.

To obtain the various parameters in Eq. 1, the Seebeck coefficient, thermal conductivity, and electrical resistivity were measured from 300 K to 400 K. In determining the Seebeck coefficient $\alpha = \Delta V/\Delta T$ at a given temperature, a longitudinal direct-current (DC) steady-state method was employed. A pair of T-type thermocouples was attached to opposite ends of a sheet-like sample. One end was heated by a resistive heater controlled by a LabVIEW graphical program, which generated a temperature difference of the order of 0.5 K to 1 K. The resulting thermo-emf was continuously recorded by a digital voltmeter as ΔT was varied. The Seebeck coefficient for the fixed temperature was obtained from the slope of a ΔV versus ΔT plot.

The thermal conductivity κ was derived from the relation, $\kappa = dDc$, with d, D, and c representing the thermal diffusivity, density, and specific heat, respectively. The thermal diffusivity was obtained using a laser flash method (LFA 457, NETZSCH), the specific heat by differential scanning calorimetry (DSC), and the density by the Archimedes method.

The electrical resistivity was measured by the standard four-probe method using a physical property measurement system (PPMS) from Quantum Design.

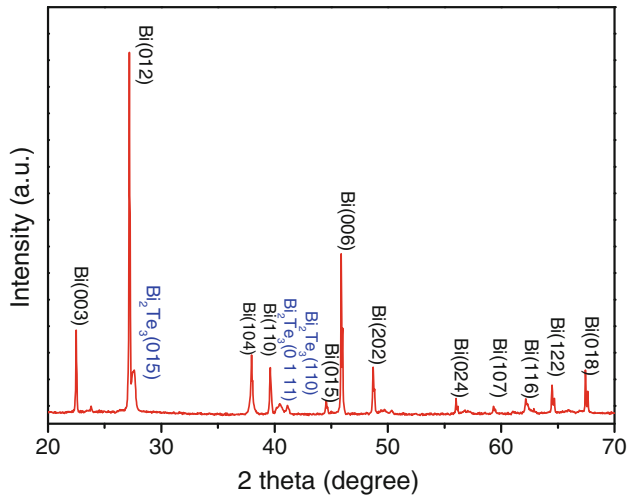

Fig. 1. X-ray diffraction patterns of hydrothermally Te-coated Bi powders (10 μm to 150 μm).

Table I. List of samples and their thermoelectric *ZT* values at 300 K, derived from Eq. 1 and experimentally obtained Seebeck coefficient, electrical resistivity, and thermal conductivity values

Sample (Bi Particle Size)	α (μV/K)	ρ ($\mu\Omega$ m)	κ (W/m K)	Density, *D* (g/cm^3)	*ZT*
Bi composite reference (10 μm to 150 μm)	−80.5	3.19	6.51	9.77 (99.8%)[a]	0.094
Sample A (10 μm to 150 μm)	−93.3	2.75	5.37	9.68 (98.9%)	0.169
Sample B (36 μm to 45 μm)	−76.4	2.67	3.02	9.78 (99.9%)	0.217
Sample C (<36 μm)	−81.8	3.03	2.39	9.70 (99.1%)	0.277

[a]Density of bulk bismuth: 9.79 g/cm^3.

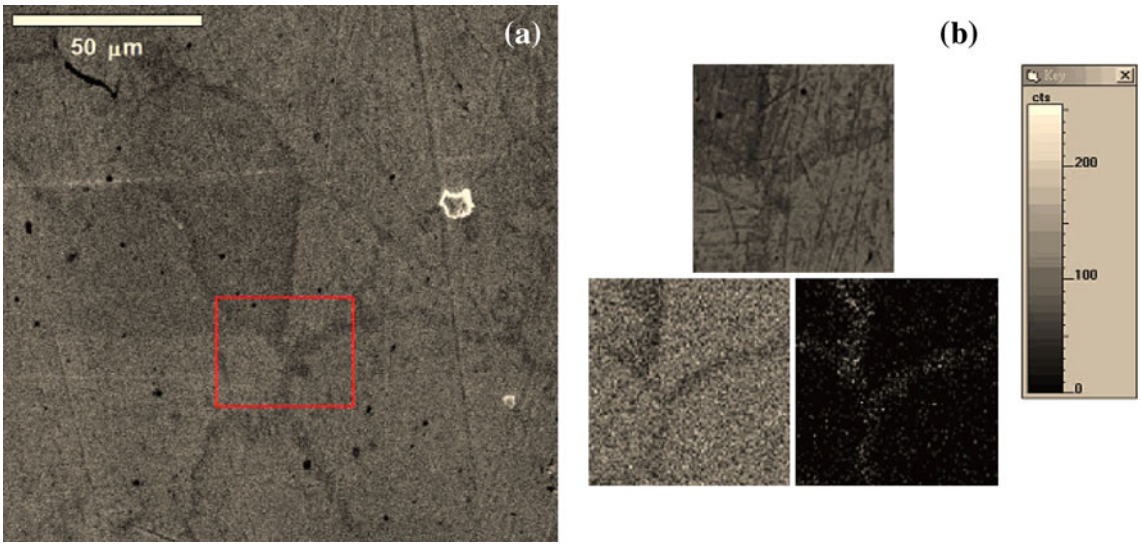

Fig. 2. (a) SEM micrograph of Bi_2Te_3–Bi composite (10 μm to 150 μm) showing grain boundaries. (b) Top: enlarged micrograph of selected area in (a); bottom left: EDS mapping of Bi; bottom right: EDS mapping of tellurium along the grain boundary of Bi particles; right: Te analysis of EDS mapping.

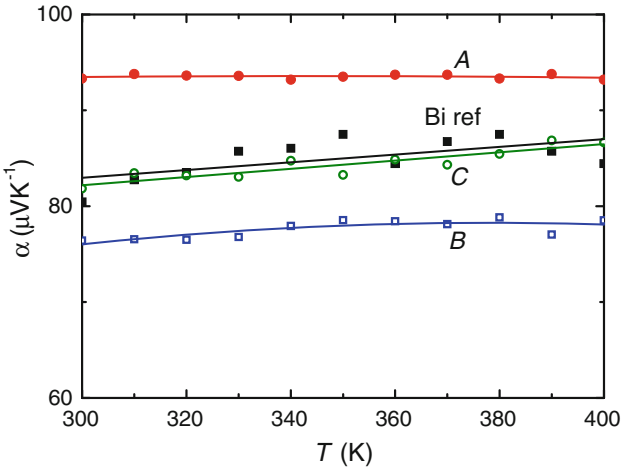

Fig. 3. Temperature and size dependence of TE properties: Seebeck coefficient.

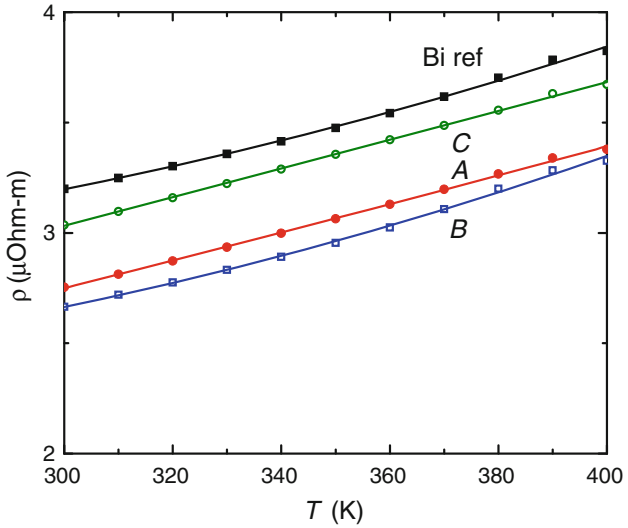

Fig. 4. Temperature and size dependence of TE properties: resistivity.

Table I summarizes the experimentally obtained values of various thermoelectric-related properties at 300 K. Also of interest for discussion are their individual temperature and particle size dependences, as illustrated in Figs. 3–6.

The semimetallic bismuth has Seebeck coefficient of -100 μV/K, while Bi_2Te_3 is an n-type semiconductor with $\alpha = -250$ μV/K. All composites in this work are also n-type, as indicated by their negative Seebeck values. Considering the small percentage of Bi_2Te_3 in the bismuth matrix, one would expect a corresponding increase of α in the tellurium-containing samples over that of the bismuth reference. No clear trend in this respect is seen in Fig. 3a, but the overall spread of α values among the four samples is relatively small compared with the other parameters in Eq. 1. This reflects additional factors beyond the particle size here. For thinly coated materials, there could easily be different degrees of off-stoichiometry in the nominally Bi_2Te_3 layer for different particles. This would in turn modify the band structure. Through an energy dependence of σ on the rate of change of electronic density of states $D(E)$, d[ln $D(E)$]/dE at the Fermi level, an additional density-of-states effect could then yield the observed behavior.

The positive but small temperature dependence of electrical resistivity for all samples shown in Fig. 3b is similar to that of the semimetallic bismuth near the borderline of semiconductors. Although

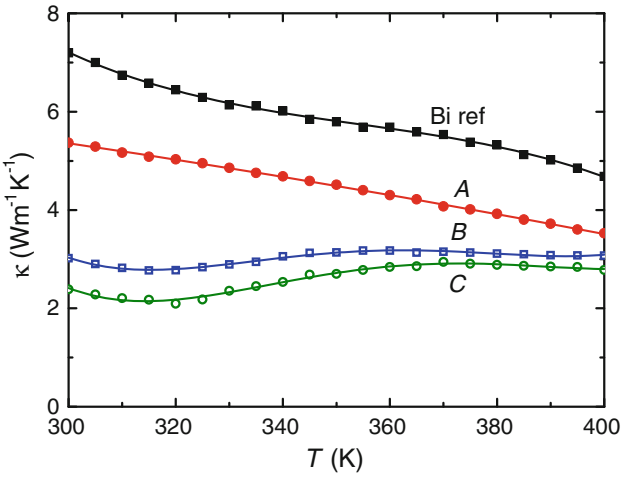

Fig. 5. Temperature and size dependence of TE properties: thermal conductivity.

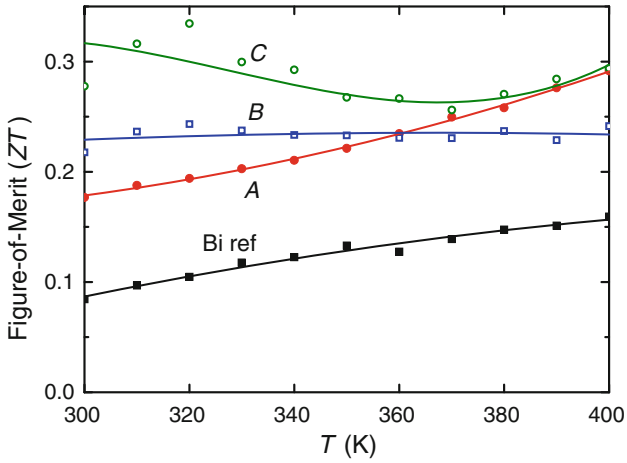

Fig. 6. Temperature and size dependence of TE properties: figure of merit *ZT*.

samples A, B, and C have extra Bi_2Te_3 interlayers at grain boundaries, their electrical resistivity in Fig. 3b is surprisingly smaller than that of the bismuth composite reference. Such a decrease in electrical resistivity could be induced by the hot-pressing process, during which Bi_2Te_3 layers act as a binder, filling voids and thus warranting better intergrain electric contact. Sample C, having the smallest size of less than 36 μm, shows higher resistivity than samples A and B. This may be caused by its larger surface area, which makes it more vulnerable to surface oxidation or impurity contamination.

As shown in Fig. 3c, the thermal conductivity diminishes gradually with decreasing particle size. This reflects the increasing number of grain boundaries. The coating layers can also limit the phonon mean free path due to their small dimensions. Furthermore, the lattice mismatch at boundaries between bismuth and Bi_2Te_3 would produce significant phonon scattering. Indeed, the overall effect is most pronounced in sample C with the smallest bismuth particles. Its ambient-temperature thermal conductivity is only 38% of that of the bismuth composite reference, and 75% of that of sample B with somewhat larger particles. Meanwhile, due to the likely different temperature dependence of each of the above-mentioned factors, the resultant thermal conductivity in Fig. 3c shows different patterns of temperature dependence among the samples. The bismuth reference and sample A have monotonically decreasing thermal conductivity as temperature increases. In contrast, samples B and C with smaller particles exhibit a minimum near 320 K, and flatten off at higher temperatures.

Finally, Fig. 3d shows the figure of merit *ZT* calculated based on Eq. 1. Basically, the composites with smaller bismuth particles yield larger *ZT* values. As expected, the dominant parameter appears to be the thermal conductivity. Most importantly, an almost threefold enhancement in *ZT* is found for sample C over that of the bismuth reference. Clearly, the hydrothermal tellurium coating plays an important role.

CONCLUSIONS

This study confirms the advantage of surface coating of fine particles for enhancing the thermoelectric figure of merit *ZT*. The significant effect arises from the reduction of thermal conductivity through increased grain-boundary formation, shorter mean free path of coating-layer phonons, and large lattice mismatch. The electrical conductivity is also improved due to a void-filling mechanism. Since Bi_2Te_3 possesses more favorable thermoelectric properties than bismuth, the Bi_2Te_3 shell should also contribute somewhat to the *ZT* enhancement. Overall, the technique described herein provides a possible alternative to improve the performance of thermoelectric materials.

ACKNOWLEDGMENTS

The authors acknowledge financial support from the Academia Sinica and the National Science Council, Republic of China, under Grant No. NSC 99-2120-M-001-001.

REFERENCES

1. G.J. Snyder and E.S. Toberer, *Nat. Mater.* 7, 105 (2008).
2. Y. Lan, A.J. Minnich, G. Chen, and Z. Ren, *Adv. Funct. Mater.* 20, 357 (2010).
3. D.M. Rowe, *CRC Book on Thermoelectrics* (Boca Raton: CRC, 1995).
4. B. Poudel, Q. Hao, Y. Ma, Y. Lan, A. Minnich, B. Yu, X. Yan, D. Wang, A. Muto, D. Vashaee, X. Chen, J. Liu, M.S. Dresselhaus, G. Chen, and Z. Ren, *Science* 320, 634 (2008).
5. M.J. Graf, S.-K. Yip, and J.A. Sauls, *Phys. Rev. B* 53, 15 (1996).

6. P.N. Alboni, X. Ji, J. He, N. Gothard, J. Hubbard, and T.M. Tritt, *J. Electron. Mater.* 36, 711 (2007).
7. B.C. Sales, D. Mandrus, and R.K. Williams, *Science* 272, 1325 (1996).
8. S.R. Hostler, Y.Q. Qu, M.T. Demko, A.R. Abramson, X.F. Qiu, and C. Burda, *Superlattices Microstruct.* 43, 195 (2008).
9. L.D. Hicks and M.S. Dresselhaus, *Phys. Rev. B* 47, 16631 (1993).
10. P.G. Borzyak, V.I. Vatamanyuk, Yu.A. Kulyupin, and A.A. Chumak, *Phys. Status Solidi A* 20, 359 (1973).
11. C. Chen, Y. Chen, S. Lin, J.C. Ho, P. Lee, C. Chen, and S.R. Harutyunyan, *J. Phys. Chem. C* 114, 3385 (2010).
12. B. Zhang, J. He, X. Ji, T.M. Tritt, and A. Kumbhar, *Appl. Phys. Lett.* 89, 163114 (2006).
13. X. Ji, J. He, Z. Su, N. Gothard, and T.M. Tritt, *J. Appl. Phys.* 104, 034907 (2008).